

Novel insights into host-pathogen interactions of large yellow croakers (*Larimichthys crocea*) and pathogenic bacterium *Pseudomonas plecoglossicida* using time-resolved dual RNA-seq of infected spleens

Yi Tang¹, Ge Xin¹, Ling-Min Zhao¹, Li-Xing Huang¹, Ying-Xue Qin¹, Yong-Quan Su², Wei-Qiang Zheng², Bin Wu³, Nan Lin³, Qing-Pi Yan^{1,2,*}

¹ Fisheries College, Key Laboratory of Healthy Mariculture for the East China Sea, Ministry of Agriculture, Jimei University, Xiamen, Fujian 361021, China

² State Key Laboratory of Large Yellow Croaker Breeding, Ningde Fufa Aquatic Products Co., Ltd., Ningde, Fujian 352000, China

³ Fujian Provincial Fishery Technical Extension Center, Fuzhou, Fujian 350003, China

ABSTRACT

Host-pathogen interactions are highly complex, involving large dynamic changes in gene expression during infection. These interactions are fundamental to understanding anti-infection immunity of hosts, as well as the pathogenesis of pathogens. For bacterial pathogens interacting with animal hosts, time-resolved dual RNA-seq of infected tissue is difficult to perform due to low pathogen load in infected tissue. In this study, an acute infection model of *Larimichthys crocea* infected by *Pseudomonas plecoglossicida* was established. The spleens of infected fish exhibited typical symptoms, with a maximum bacterial load at two days post-injection (dpi). Time-resolved dual RNA-seq of infected spleens was successfully applied to study host-pathogen interactions between *L. crocea* and *P. plecoglossicida*. The spleens of infected *L. crocea* were subjected to dual RNA-seq, and transcriptome data were compared with those of noninfected

spleens or *in vitro* cultured bacteria. Results showed that pathogen-host interactions were highly dynamically regulated, with corresponding fluctuations in host and pathogen transcriptomes during infection. The expression levels of many immunogenes involved in cytokine-cytokine receptor, Toll-like receptor signaling, and other immune-related pathways were significantly up-regulated during the infection period. Furthermore, metabolic processes and the use of oxygen in *L. crocea* were strongly affected by *P. plecoglossicida* infection. The WGCNA results showed that the metabolic process was strongly related to the entire immune process. For *P. plecoglossicida*, the expression levels of motility-related genes and flagellum assembly-related genes were significantly up-regulated. The results of this study may help to elucidate the interactions between *L. crocea* and *P. plecoglossicida*.

Keywords: *Larimichthys crocea*; *Pseudomonas*

Open Access

This is an open-access article distributed under the terms of the Creative Commons Attribution Non-Commercial License (<http://creativecommons.org/licenses/by-nc/4.0/>), which permits unrestricted non-commercial use, distribution, and reproduction in any medium, provided the original work is properly cited.

Copyright ©2020 Editorial Office of Zoological Research, Kunming Institute of Zoology, Chinese Academy of Sciences

Received: 27 December 2019; Accepted: 31 March 2020; Online: 31 March 2020

Foundation items: This work was supported by the National Natural Science Foundation of China (31672694, 31972836), and Fujian Provincial Special Fund for Marine and Fishery Protection and Development (MCZ[2019]062)

*Corresponding author, E-mail: yanqp@jmu.edu.cn

DOI: 10.24272/j.issn.2095-8137.2020.035

plecoglossida; Dual RNA-seq; Host-pathogen interactions; Dynamic transcriptome

INTRODUCTION

Large yellow croakers (*Larimichthys crocea*), a marine fish with the largest annual yield in China, are widely cultured in Fujian and Zhejiang provinces (Sun et al., 2019a; Yang et al., 2016). The most significant factor affecting the production of *L. crocea* is the frequent outbreak of diseases caused by pathogens (Tang et al., 2019a). The “visceral white spot disease” caused by *Pseudomonas plecoglossida* is one of the most destructive diseases of *L. crocea*, causing considerable economic losses (Huang et al., 2018; Zhang et al., 2014). This pathogen not only infects large yellow croakers but is the causative agent of bacterial hemorrhagic ascites disease in *Plecoglossus altivelis* (Nishimori et al., 2000). In a previous study, *P. plecoglossida* infection (10^4 colony forming units per gram (cfu/g)) resulted in 100% *L. crocea* death rate at 4.5 days post-injection (dpi) (Tang et al., 2019c), indicating that *P. plecoglossida* is more virulent than most other aquatic pathogens, including *Vibrio alginolyticus* (Huang et al., 2017; Liu et al., 2017) and *Aeromonas hydrophila* (Zhang et al., 2018b, 2019c). In view of the considerable damage caused by *P. plecoglossida* to aquaculture, its pathogenic mechanism has attracted the attention of researchers (Huang et al., 2018; Tao et al., 2016), resulting in the identification of several virulence genes (Luo et al., 2019a; Zhang et al., 2019a).

Infection is a life-and-death struggle between host and pathogen (Zhang et al., 2018a), in which both pathogen and host must mobilize all available resources to win (Luo et al., 2020). Many of the changes that occur in pathogens and hosts during infection will be reflected in their respective transcriptome profiles (Jenner & Young, 2005; Sorek & Cossart, 2010). Traditional RNA-seq has been widely used (Sun et al., 2018; Yang et al., 2018) but cannot detect both host and pathogen transcriptomes simultaneously. However, dual RNA-seq provides analysis of both host and pathogen transcriptome interactions, providing valuable insights into infectious biology (Westermann et al., 2012, 2017). Dual RNA-seq has been used in many bacterial infection studies, including cell-infected and animal-infected models, and has identified many key genes involved in pathogen-host interactions (Aprianto et al., 2016; Minhas et al., 2019; Westermann et al., 2016). For instance, analysis of host and pathogen transcriptional profiles during *Staphylococcus aureus* infection of two mouse strains demonstrated that the expression of virulence factors is dependent on encountered host resistance (Thänert et al., 2017). Furthermore, using a murine model of pneumococcal infection, Ritchie & Evans (2019) identified key host and bacterial responses to invasion of the pleural space. Dual RNA-seq has also been used to study virulence genes in host-pathogen interactions. (Sun et al., 2019a; Wang et al., 2019). Furthermore, recent study integrated dual RNA-seq and dual iTRAQ (Luo et al., 2019b).

Host-pathogen interactions are a complex dynamic process. To date, however, most dual RNA-seq studies of infected tissue have been obtained through static dual RNA-seq (Luo et al., 2020).

To better understand the interactions of *L. crocea* and *P. plecoglossida*, an infection model was established, and the spleens at different stages of infection were subjected to dual RNA-seq to simultaneously monitor the transcriptomes of both *L. crocea* and *P. plecoglossida*. The results of this study should help elucidate host-pathogen interactions between *L. crocea* and *P. plecoglossida*.

MATERIALS AND METHODS

Experimental fish and temporary culture conditions

All healthy and size-matched *L. crocea* were provided by the State Key Laboratory of Large Yellow Croaker Breeding, Ningde, China. The fish were acclimatized at 18 ± 1 °C for one week under specific pathogen-free laboratory conditions before infection.

Bacterial strain and culture conditions

The pathogenic *P. plecoglossida* (NZBD9) strain was isolated from the spleen of naturally infected *L. crocea* (Huang et al., 2018). The bacteria were routinely overnight cultured in Luria Bertani (LB) broth at 18 or 28 °C with shaking at 220 r/min.

Infection test

All fish experiments were carried out in strict accordance with the "Guide for the Care and Use of Laboratory Animals" established by the National Institutes of Health. All animal protocols were approved by the Jimei University Animal Ethics Committee (Acceptance No. JMULAC201159).

For survival assays, acclimatized *L. crocea* were injected intrapleurally with 10^4 cfu/g of *P. plecoglossida* (NZBD9) (Tang et al., 2019c). The *L. crocea* fish intrapleurally injected with 0.1 mL of phosphate-buffered saline (PBS) were used as a negative control. The water temperature during the entire experiment was maintained at 18 °C. The mortality of infected *L. crocea* was recorded twice a day. Dead *L. crocea* were removed in a timely manner, and their spleens were dissected and photographed.

For dual RNA-seq assays, the spleens of six infected *L. crocea* were sampled at 1, 2, 3, and 4 dpi. Two spleens were mixed as one sample. PBS-treated *L. crocea* and *in vitro*-cultured *P. plecoglossida* (18 °C) were used as controls.

RNA isolation, cDNA library construction, and sequencing

Total RNA of spleens and *P. plecoglossida* strains was extracted separately using TRIzol reagent (Invitrogen, USA). Turbo DNA-free DNase (Ambion, USA) treatment was performed to remove possible contaminant genomic DNA. The RNA samples were further purified using a Ribo-Zero rRNA Removal Kit (human/mouse/rat or gram-negative bacteria) (Epicentre, USA). The mRNA samples were then fragmented in fragmentation buffer, and a SuperScript double-stranded

cDNA synthesis kit (Invitrogen, USA) was used to synthesize cDNA. After modification and purification, library fragments were enriched by polymerase chain reaction (PCR) amplification. An Agilent 2100 Bioanalyzer (Agilent Technologies, USA) was used to detect library quality. The Illumina NovaSeq sequencing platform was used to carry out second-generation sequencing.

Transcriptome data analysis

Sequence data processing and differential gene expression analysis: The measurement of differential gene expression was performed individually for the *P. plecoglossicida* and *L. crocea* libraries. Read mapping and transcript abundance quantification (FPKM-normalized expression value) were performed using Bowtie2 (Kim et al., 2015) and RSEM (Li & Dewey, 2011). Differentially expressed mRNAs (DEMs) at different time points were tested using the package edgeR with $FDR < 0.05$ & $|\log_2 \text{fold-change}| \geq 1$. ClusterProfiler and Goatools were used for Gene Ontology (GO) enrichment analysis of *L. crocea* and *P. plecoglossicida*, respectively, and only categories with $P < 0.05$ were considered to be enriched in the network (Klopfenstein et al., 2018; Yu et al., 2012). The Kyoto Encyclopedia of Genes and Genomes (KEGG) database was used for pathway enrichment analysis (Kanehisa & Goto, 2000).

STEM analysis: To analyze changes in gene expression in different infection time samples, Short Time-series Expression Miner (STEM) (v1.3.11) was used to analyze gene expression patterns in *L. crocea* and *P. plecoglossicida* (Ernst & Bar-Joseph, 2006). As recommended by the software, the median FPKM in the biological repeat group was selected as the final expression amount. Clustered profiles with $P < 0.05$ were considered significantly expressed, and DEMs were clustered into different expression patterns for subsequent analysis.

Weighted gene co-expression network analysis: Weighted gene co-expression network analysis (WGCNA) was performed on *L. crocea* and *P. plecoglossicida* data using the WGCNA package in R (Langfelder & Horvath, 2008). WGCNA can help identify functional pathways when studying species interactions (Grote et al., 2017). Ranked by variance from large to small, we chose the top 25% of genes for WGCNA. A network was created based on the results of the pickSoftThreshold function. Hierarchical clustering and dynamic branch cutting were used to identify stable modules of densely interconnected genes. Hub genes were defined by module connectivity, as measured by the absolute values of Pearson's correlations. Hub genes in a module are considered to have significant functional significance. In this study, key modules were visualized by Cytoscape (<http://www.cytoscape.org/>).

Quantitative real-time PCR (qRT-PCR)

To confirm the accuracy of data obtained with dual RNA-Seq, some DEMs from bacteria and fish were randomly selected for qRT-PCR. All primers used are listed in Supplementary Table S2. Primers were designed by Primer Premier 5.0 (Premier Biosoft International, Palo Alto, CA, USA). qRT-PCR was

performed using QuantStudio 6 Flex (Life Technologies, USA). Three replicates were included for each sample, and the β -actin gene of *L. crocea* served as an internal control to normalize the expression levels; for bacteria, 16S was used for normalization (Wang et al., 2019). The $2^{-\Delta\Delta Ct}$ method was used to calculate the relative level of differential gene expression (Livak & Schmittgen, 2001). All data represent the mean \pm standard deviation (SD) of three replicates.

Bacterial load determination

DNA purification from spleens was accomplished with an EasyPure Marine Animal Genomic DNA Kit (TransGen Biotech, China) following the manufacturer's instructions. The abundance of *P. plecoglossicida* was estimated by qRT-PCR using the copy number of the gyrB gene (Huang et al., 2019). Three replicates were conducted for each experiment.

Statistical analyses

Data are expressed as means \pm SD. Data analysis was performed with SPSS 17.0 (SPSS Inc., USA). Independent sample *t*-test and one-way analysis of variance (ANOVA) with Dunnett's test were used. *P*-values less than 0.05 were considered significant.

Data access

The RNA sequencing read data were deposited in the GenBank SRA database under accession Nos. SRP176599 and PRJNA597434.

RESULTS

Pathogen load in spleen after infection

As the causative agent of "visceral white spot disease" in *L. crocea*, *P. plecoglossicida* exhibited strong pathogenicity to *L. crocea*. After intrapleural injection of a relatively low dose (10^4 cfu/g) of *P. plecoglossicida*, experimental fish died shortly thereafter. The first death of *L. crocea* was recorded at 2.5 dpi, and the last death was recorded at 4.5 dpi (Tang et al., 2019c). All *L. crocea* counterparts from the CG that received intrapleural injections of PBS survived the experimental period.

At 3 dpi, the spleens in *L. crocea* injected with *P. plecoglossicida* exhibited typical symptoms (spleen surface covered with numerous white spots); however, no white spots were observed on the surface of spleens in the *L. crocea* CG (Figure 1A).

The qRT-PCR results showed that the *P. plecoglossicida* load in the infected spleens varied with time of infection. At the beginning of infection, the bacterial load was notably low, then increased rapidly, peaked at 2 dpi, and decreased with time (Figure 1B).

Transcriptome of infected spleens reflects different temporal dynamics during infection

An overview of sequencing and mapping results of *L. crocea* and *P. plecoglossicida* in infected spleens is provided in Supplementary Table S1. Principal component analysis (PCA)

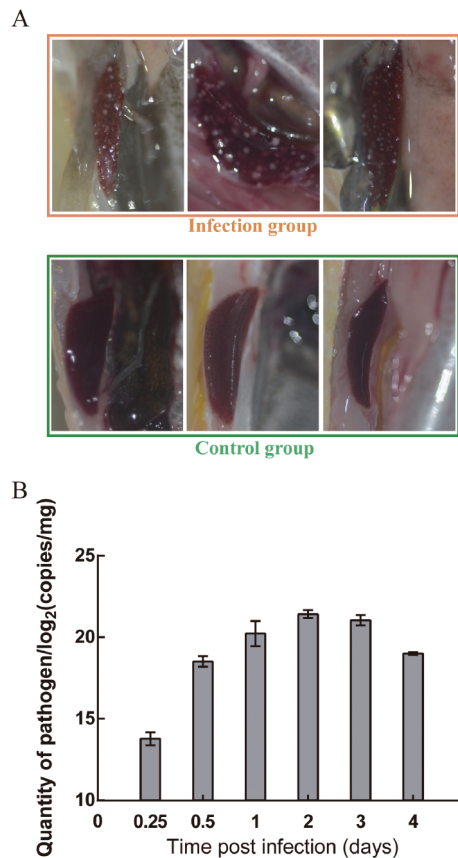


Figure 1 Pathology and pathogen load in spleen of *L. crocea* infected by *P. plecoglossicida* NZBD9

A: Symptoms of spleens. Infection group was injected with *P. plecoglossicida*, and control group (CG) was injected with PBS. B: Pathogen load of *P. plecoglossicida* in infected *L. crocea*.

of fish samples revealed a major difference between infected and uninfected samples (Figure 2A). Fish transcript profiles from infected samples could be further assigned into two groups: WT1d and WT2d–WT3d–WT4d (13.17% of variance; Figure 2A). Similarly, PCA analysis of *P. plecoglossicida* transcript profiles identified two groups (Figure 2B). Some host and pathogen genes were randomly chosen for qRT-PCR, with results demonstrating the reliability of dual RNA-seq data. Fold-changes obtained by qRT-PCR and dual RNA-seq showed a relatively high correlation for both species: $R^2=0.7561$ for host transcripts and $R^2=0.749$ for pathogenic transcripts (Figure 2C), validating the reliability of the dual RNA-seq data. The main expression of the transcriptomes of the two species is shown in Figure 2E, D.

Infection-induced changes in gene expression of *L. crocea*

To analyze the dynamic changes in the host transcriptome during infection, we performed multiple transcriptome comparisons and subsequent analysis. The number of DEMs between any two transcriptomes (CG, WT1d, WT2d, WT3d,

WT4d) of *L. crocea* is shown in Figure 3A. The comparison group with the largest difference in each column was the CG and infected group.

There was a clear difference in the number of DEMs between the WT1d, WT2d, WT3d and WT4d groups compared with the control. Therefore, we used GO and KEGG enrichment analysis to determine the biological function of the identified DEMs. The GO enrichment analysis results in biological process (BP) and molecular function (MF) are shown in Figure 3B. Compared with the CG, the GO terms enriched in all infected groups were peptide metabolic process, translation, peptide biosynthetic process, protein heterodimerization activity, structural constituent of ribosome, and protein dimerization activity. These terms are mainly related to protein synthesis. An immunologically related term (GO: 0006955: immune response) could be seen after 3 dpi. Notably, many GO terms related to nucleic acid synthesis were enriched only on the second day (Figure 3B). However, on the second day, many fish deaths occurred after infection.

The KEGG enrichment results showed that the ribosome pathway was significantly enriched in the WT1–4d groups (Figure 3C). The infection-related pathway (Herpes simplex virus 1 infection) was enriched, except in WT1d, whereas WT3d and WT4d were enriched in pathways related to host defense, such as the Toll-like receptor signal pathway and cytokine-cytokine receptor interaction.

Infection is a dynamic process. To use time series information effectively, gene expression pattern clustering was applied to mine the expression rule of genes. In the STEM profile, some specific expression patterns appeared due to the influence of biological laws, but some were random. To remove this, we calculated the *P*-value of each profile through a specific statistical model, with $P<0.001$ considered to be an authentic and useful research profile.

A total of 50 profiles were aggregated, but only 11 highly significant expression profiles were selected for subsequent analysis ($P<0.001$), as shown in Supplementary Figure S1A. We used the same color to represent similar expression patterns (Figure 4). Compared with the CG, the profiles of 18-LC, 41-LC, and 43-LC, in which mRNAs were largely up-regulated, are shown in red. The mRNAs in green showed overall down-regulation, but with an up-regulation trend. The mRNAs in purple and yellow modules were generally down-regulated but fluctuated, whereas the mRNAs in the orange profile were generally up-regulated and stable.

To determine the biological function of DEMs in each profile, GO classification and KEGG pathway analysis were carried out. From the GO MF enrichment results in Figure 5A, no overlap was observed in GO terms for any profile. Different expression patterns corresponded to different biological processes. The DEMs in profile 0-LC were enriched with many oxygen-related GO terms, whereas profile 38-LC was enriched with many protein-related terms. For the genes in other profiles, a large number were dominant in enzyme activity, binding, and energy.

KEGG pathway analysis showed that the DEMs in eight

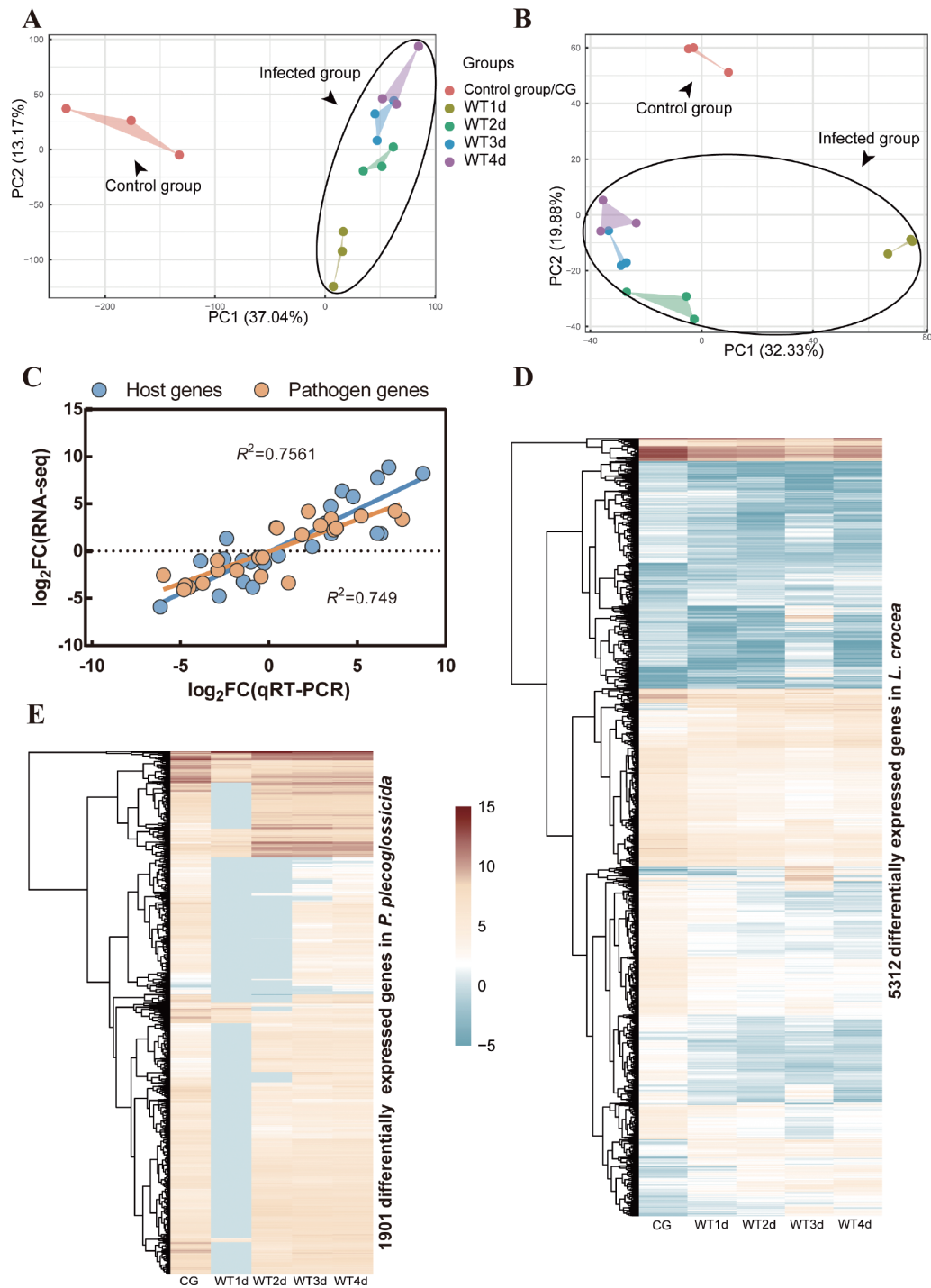


Figure 2 Transcriptional profiles of *L. crocea* and *P. plecoglossicida* in infected spleens

A: PCA clustering of full transcriptional profiles of *L. crocea*. B: PCA clustering of full transcriptional profiles of *P. plecoglossicida*. C: Validation of RNA-seq data by qRT-PCR. Blue indicates host, orange indicates pathogen, and R-square is marked. D: Hierarchical clustering of major classes of differentially expressed mRNAs (DEMs, $P < 0.01$, \log_2 fold-change (Log_2FC) ≥ 2) in *L. crocea* transcriptomes. E: Hierarchical clustering of major classes of DEMs ($P < 0.01$, \log_2 fold-change (Log_2FC) ≥ 2) in *P. plecoglossicida* transcriptomes. Relative expression levels of each transcript (rows) in each sample (column) are shown. FPKM was \log_2 -transformed and then median-centered by transcript. CG: Control group; WT1d: Infected group sampled at 1 dpi; WT2d: Infected group sampled at 2 dpi, and so on. Same below.

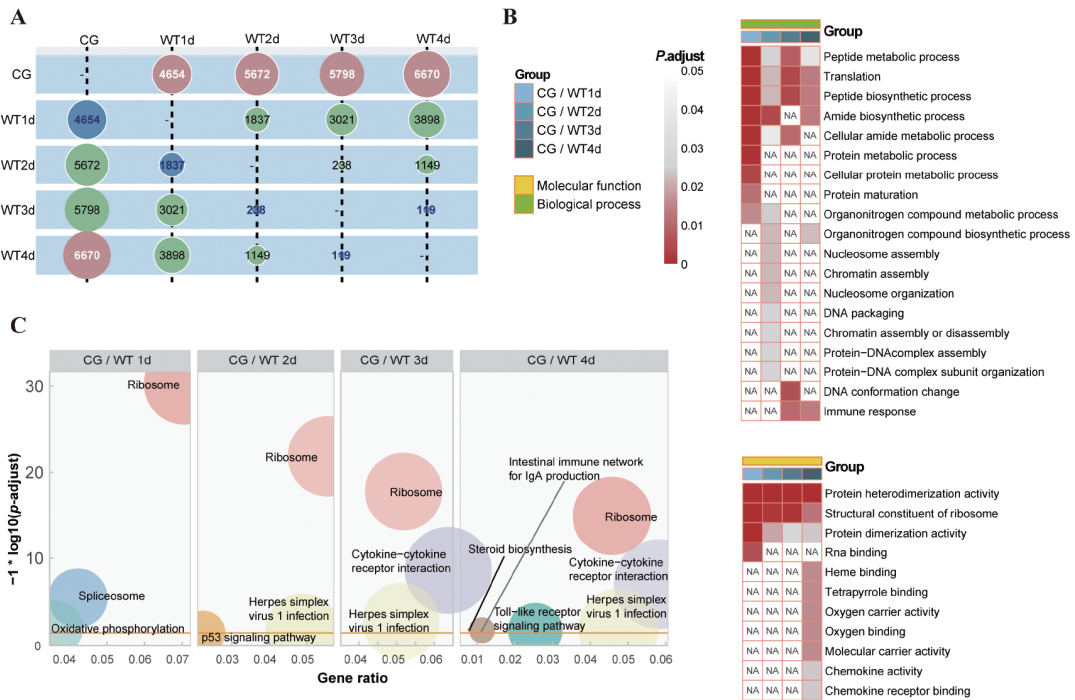


Figure 3 Differentially expressed mRNA (DEM) analysis of *L. crocea* infected by *P. plecoglossida*

A: Numbers of DEMs between time points in host. Most different time point across all comparisons (i.e., within a column) is shown in red, most similar time point across all comparisons (i.e., within a column) is shown in blue. B: Heat map of GO enrichment analyses. Shade of color represents size of P -adjusted value, "NA" indicates not significantly enriched in this comparison group. C: KEGG enrichment analysis. Size of circle represents size of enriched gene number, each color represents a pathway.

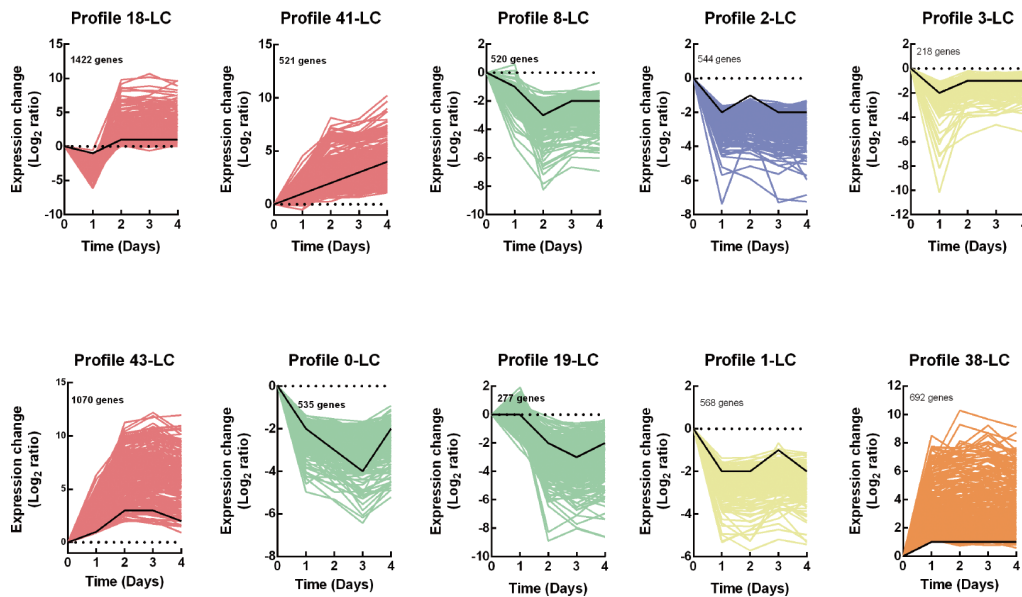


Figure 4 Trend analysis of DEM enrichment across infectious stages of *L. crocea*

Ten gene sets clustered by STEM software. Control group (CG) was represented by 0 d, and top left corner shows number of genes in profile.

profiles were mapped with 19 pathways, as shown in Figure 5B, e.g., profile 0-LC, profile 1-LC, profile 2-LC, and

profile 3-LC. There were multiple profiles enriched with ribosomes and spliceosomes. Notably, profile 43-LC was

enriched in immune-related pathway cytokine-cytokine receptor interaction.

Host adaptation of *P. plecoglossida* to *L. crocea*

Figure 6A shows the number of differentially expressed genes

between any two transcriptomes (CG, WT1d, WT2d, WT3d, WT4d) of *P. plecoglossida*. Compared with the CG, WT3d had the greatest number of DEMs in the infected group, reaching 2 115.

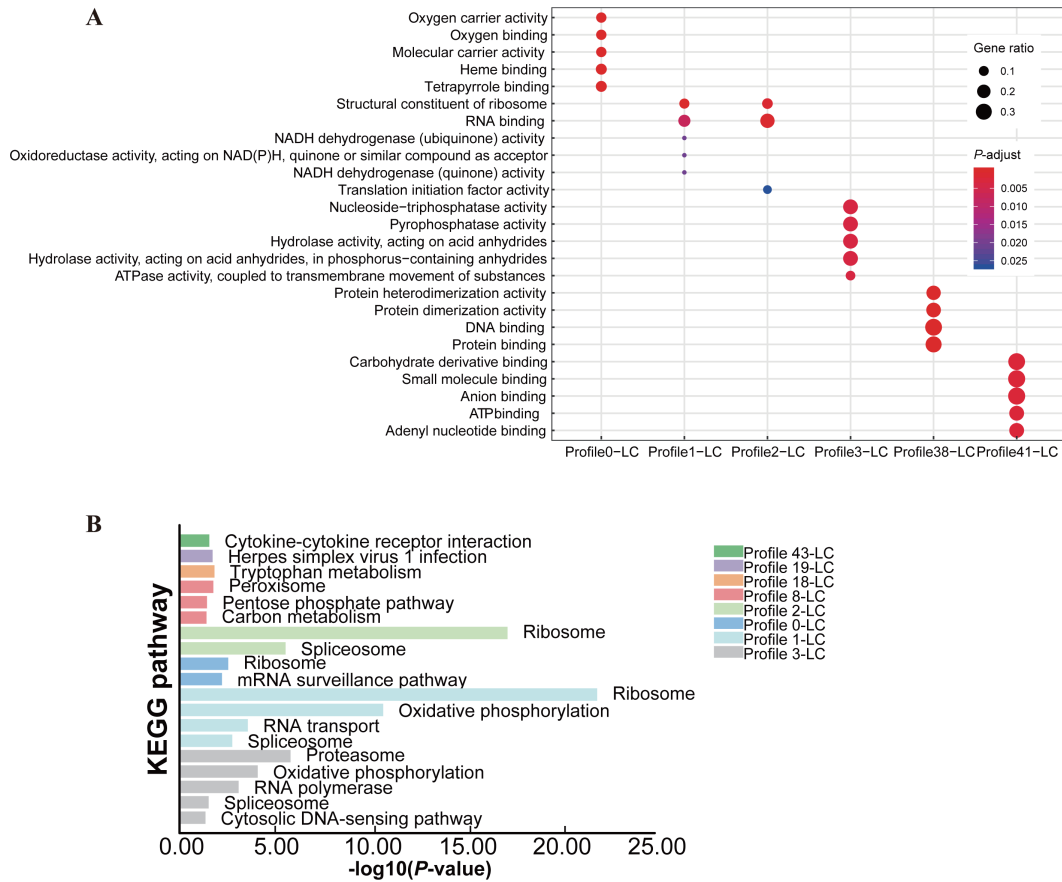


Figure 5 STEM profile enrichment analysis of *L. crocea*

A: Top five GO molecular function (MF) terms for six profiles. Size of circle represents number of enriched genes, each color indicates significance. B: KEGG pathway enrichment analysis. Different colors are used to represent different profiles, and height of bar graph indicates significance.

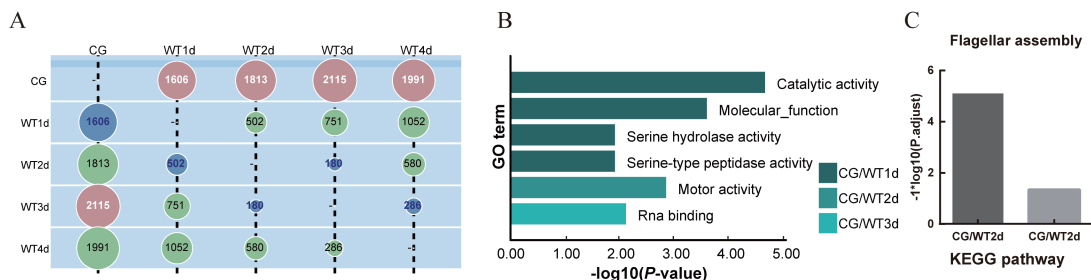


Figure 6 Differentially expressed mRNA (DEM) analysis of *P. plecoglossida*

A: Numbers of DEMs between time points in host. Most different time point across all comparisons (i.e., within a column) is shown in red, most similar time point across all comparisons (i.e., within a column) is shown in blue. B: GO molecular function (MF) enrichment analyses. Different colors represent different groups, and length of bar graph indicates significance. C: KEGG enrichment analyses.

Compared with the CG, the results of GO enrichment are shown in Figure 6B. The CG/WT1d group was dominated by catalytic activity, the CG/WT2d group was related to motor activity, and the CG/WT3d group was related to RNA binding.

For KEGG enrichment, only the CG/WT2d and CG/WT3d groups had results, and they were all related to flagellar assembly and bacterial chemotaxis (Figure 6C).

To analyze the expression mode of DEMs, which played key roles in the infection process, we performed trend analysis of DEMs from the five transcriptomes. A total of 50 profiles were aggregated, with nine highly significant expression profiles then selected for subsequent analysis ($P < 0.001$), as shown in Figure 7 and Supplementary Figure S1. Compared with the CG, the expression levels of genes in modules 18-PP, 43-PP, and 41-PP were generally up-regulated, whereas gene expression levels in modules 3-PP, 1-PP, 0-PP, and 8-PP were down-regulated. For genes in modules 14-PP and 5-PP, gene expression was first down-regulated and then up-regulated.

The dynamic process of *P. plecoglossicida* during infection was elucidated by GO enrichment analysis of expression profiles. Some profiles did not show useful results; therefore, only 18-PP, 43-PP, 41-PP, 5-PP, 3-PP, and 1-PP (Figure 7A)

were selected for analysis. The module which enriched the most GO terms was profile 18-PP. Compared with the CG, gene expression decreased on the second day, but was up-regulated thereafter. The GO terms enriched in profile 18-PP were mainly related to ribosomes, transcriptional translation, or energy. The top 10 GO terms are shown in Figure 7C. These GO terms were both necessary and fundamental to pathogen activity.

As shown in Figure 7B, only the enriched GO terms in module 43-PP were related to bacterial movement and flagella: i.e., bacterial-type flagellum-dependent cell motility; cilium or flagellum-dependent cell motility; archaeal or bacterial-type flagellum-dependent cell; motility; cell motility; movement of cell or subcellular component; and bacterial-type flagellum part and locomotion. Based on STEM profiles, the general expression of a gene can be observed. Compared with the CG, the genes in profile 43-PP showed an upward trend until the fourth day, after which gene expression began to decrease slightly when most of the hosts died (Figure 7A). Thus, we speculate that flagella were important for *P. plecoglossicida* throughout the infection period.

The GO enrichment results of profiles 3-PP and 1-PP are shown in Figure 7B. The expression patterns of these two

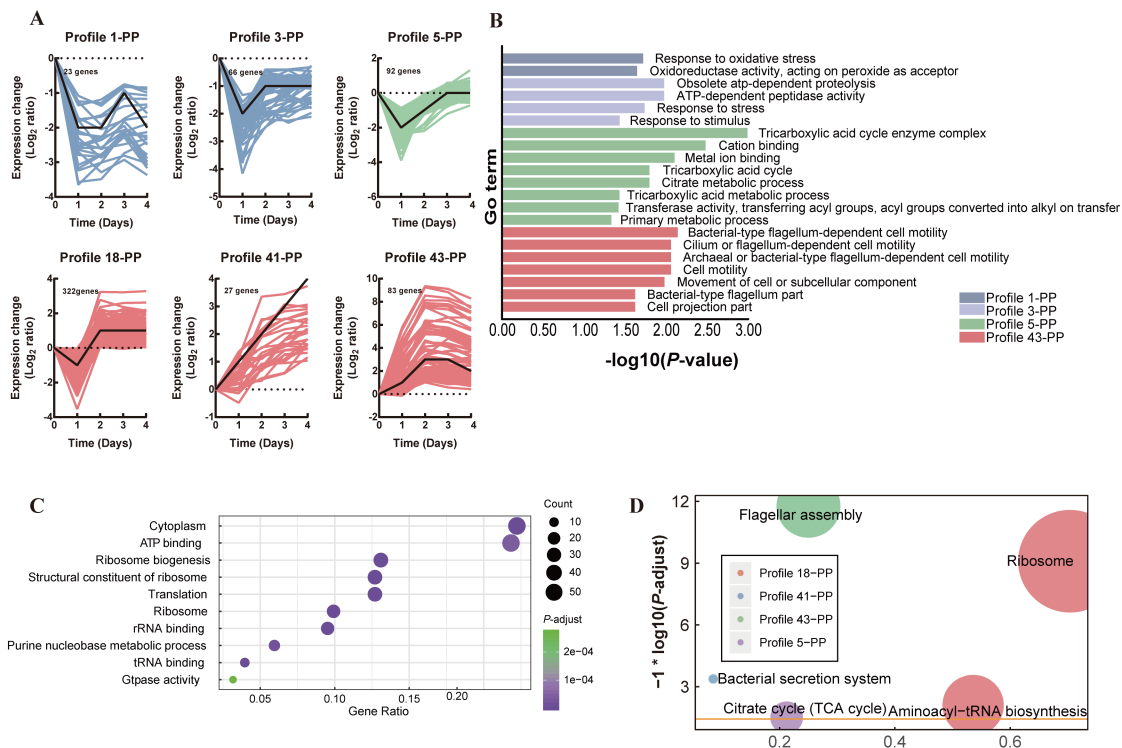


Figure 7 STEM analysis for *P. plecoglossicida*

A: Six major profiles of gene expression. Top left-hand corner indicates number of DEMs belonging to profile. Lower left-hand corner shows P -value of profile. Colored lines represent DEMs. X-axis represents days after *P. plecoglossicida* inoculation (dpi). Y-axes represent \log_2 -fold-change in gene expression between treatments. B: GO enrichment analysis of profile 43-PP, 5-PP, 3-PP, and 1-PP. C: Top ten GO terms of profile 18-PP. Size of circle represents quantity of enriched genes, and each color indicates significance. D: KEGG pathway enrichment analysis. Size of circle represents size of enriched gene number, each color represents different groups.

profiles were similar, and showed enrichment in resistance-related GO terms: i.e., response to stress and response to stimulus.

Co-expression of host and pathogen genes

To determine which genes were co-expressed between *L. crocea* and *P. plecoglossicida* during infection, we built a co-expression network for the two organisms using WGCNA (Figure 8). In the same module, co-expressed genes at different time points were identified. In total, the CG and four experimental groups contained 15 samples, with variance then calculated. The top 25% of genes were used to construct the gene co-expression network. The choice of soft-thresholding power was an important step in building a co-expression network. We performed network topology analysis of the soft-thresholding power from 1 to 20 and determined the relative balance of scale independence and average connectivity of the network. The middle results are shown in Supplementary Figure S2.

To determine the importance of the modules for our research, we performed enrichment analysis on each module. The yellow module was enriched in many immune-related pathways, as shown in Figure 8B. Therefore, the yellow module was believed to be most important for the infection process. The pathogenic genes in this module were enriched

in two meaningful pathways, i.e., flagellar assembly and bacterial chemotaxis.

To understand host-pathogen interactions, we selected several key genes for analysis. We calculated the KME values of genes in the yellow module and selected genes with $KME > 0.8$ and $weight > 0.35$ for visualization. The interaction diagram is shown in Figure 8C. Only five bacterial genes qualified: i.e., *dadA*, *aldH*, *dapA*, *L321_RS03170*, and *L321_RS20070*.

DISCUSSION

The low load of pathogens is one of the main limiting factors in the application of dual RNA-seq (Luo et al., 2019b). The spleen is not only an important immune organ for fish (Chen et al., 2019) but also a major target organ for *P. plecoglossicida* infection (Zhang et al., 2018a). The pathogen load of *P. plecoglossicida* in the spleen is two or three orders of magnitude higher than that of other organs (Luo et al., 2020). The *P. plecoglossicida*-infected spleen was chosen for dual RNA-seq, not only because of its high pathogen load, thus meeting the requirements of dual RNA-seq, but also because it can reflect interactions between host and pathogens. In addition, the infected spleen has been used in previous studies on interactions between *P. plecoglossicida* and host

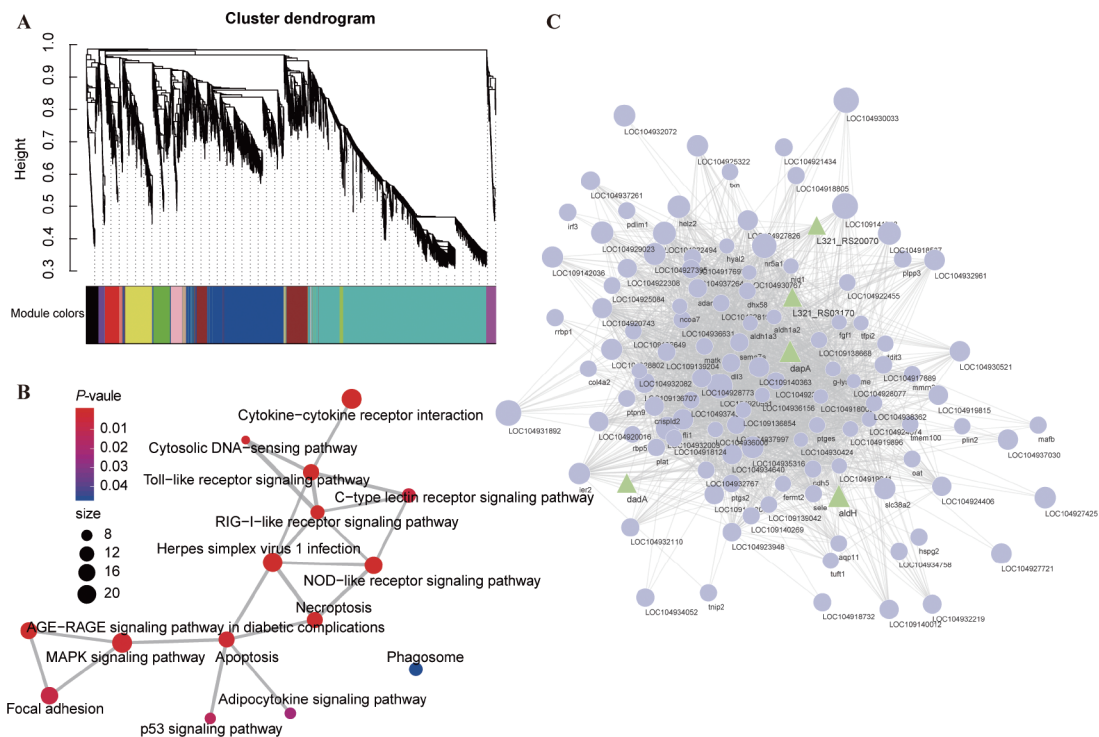


Figure 8 Weighted Gene Co-expression Network Analysis (WGCNA) of transcriptional changes in *L. crocea* and *P. plecoglossicida*

A: *L. crocea* time-resolved transcriptome WGCNA cluster map. B: KEGG enrichment analysis for yellow module. Size of circle represents number of genes in pathway, color indicates significance, and connected pathways represent genes within it. C: Correlation network of genes in yellow module, *L. crocea* and *P. plecoglossicida* genes with edge weights greater than 0.35. Dot size represents KME values. *L. crocea* genes are shown in purple, *P. plecoglossicida* genes are shown in green.

(Sun et al., 2019b; Tang et al., 2019b).

Both the heat map of the major DEMs and PCA analysis showed that the transcriptome changes during infection were enormous. The number of DEMs plot shows the fluctuations and consistency of changes in *L. crocea* and *P. plecoglossicida* during infection. The changes in each period of infection were different, as shown in Figures 3, 6. Immune-related GO terms were enriched in the host after 3 dpi, whereas GO functional enrichment results for pathogens differed every day. As infection time increased, the immune system became more sensitive and the immune response was more comprehensive.

As life activity is a dynamic process, time series experiments can effectively characterize the expression of genes. Different from traditional expression difference analysis, it is more crucial to screen expression patterns of interest based on cluster analysis of gene expression patterns, that is, variation in expression levels and subsequent functional enrichment analysis on genes in the given module.

Host innate immunity uses a variety of recognition receptors, such as Toll-like receptors, to identify bacteria that attack the host (Gulati et al., 2018). Transcriptome analysis of *Oreochromis niloticus* during *Streptococcus agalactiae* infection revealed that the Toll-like receptor-mediated pathway helps the immune response and protects the host against pathogens (Ken et al., 2017). Here, results showed that the expression of many genes in the Toll-like receptor signaling pathway was significantly up-regulated (Figure 3C) at the later stage of infection (4 dpi). Cytokines are key regulators of host defense in innate immunity and adaptive inflammation (Akdís et al., 2016). Gene expression within the “cytokine-cytokine receptor interaction” changed significantly at 3 dpi and 4 dpi (Figure 3C). Gene expression in module profile 43-LC, which was enriched in the “cytokine-cytokine receptor interaction” pathway based on STEM cluster analysis, was higher than that in the CG overall during infection (Figure 4). These results indicate that the immune response of *L. crocea* was enhanced during *P. plecoglossicida* infection.

A host's metabolic regulation during infection is also very important and has a significant impact on the immune response (Nhan et al., 2019). The immune system can resist pathogens and maintain tissue homeostasis for the life of the organism but requires a large investment in bioenergy (Ganeshan & Chawla, 2014). Thus, to overcome the stresses caused by pathogens, infected fish need to consume large amounts of energy (Yin et al., 2014, 2015). Amino acid metabolism is essential for consumption of energy, synthesis of detoxified protein, and safe operation of innate immune responses in fish (Lu et al., 2017; Zhang et al., 2019b). As seen from STEM analysis, gene expression in profile 18-LC decreased slightly on the first day, but overall showed an upward trend. Based on KEGG enrichment, the genes in profile 18-LC were closely related to the tryptophan metabolism pathway. We speculate that on the first day, after the fish were switched to a new environment, they reduced their consumption to adapt to the environment, accompanied

by increasingly serious infection, requiring amino acid metabolism to provide required elements such as energy and protein. Tryptophan and its metabolites play important roles in regulating immune mechanisms in marine animals, especially humoral immunity (Curti et al., 2009; Mondanelli et al., 2019). Lu et al. (2017) claimed that *Vibrio parahaemolyticus* infection can cause changes in tryptophan metabolism in female *Halotis diversicolor*, with similar phenomena also observed in zebrafish (Ji et al., 2019). Deeper infection with *Aeromonas salmonicida* is also known to reduce metabolites (including choline, glycerophosphocholine (GPC), betaine, and glycine) in the tryptophan metabolism pathway of Atlantic salmon (Liu et al., 2016).

Respiratory bursts are a basic strategy for fish species to fight against pathogens and are often accompanied by substantial oxygen consumption (Billar & Takahashi, 2018; Lu & Chen, 2019; Yilmaz, 2019). During fish immunological responses to pathogens, respiratory bursts play an important biochemical role that facilitates successful phagocytosis and eventual pathogen destruction (Lulijwa et al., 2019). In the current study, however, profile 0-LC, which showed down-regulated expression during infection, exhibited functional enrichment associated with oxygen metabolism (GO: 0005344, GO: 0019825, GO: 0020037, GO: 0005506) (Figure 4, 5); in other words, *L. crocea* was in a state of reduced breathing. Thus, *P. plecoglossicida* infection inhibited *L. crocea* respiration, which is consistent with the experimental phenomenon we observed. We speculate that this effect may be one of the main causes of death from visceral white spot disease.

For pathogens invading a host, flagella play a series of key roles, including reaching the optimal host site, colonization or invasion, maintenance at infection site, and post-infection dispersal (Chaban et al., 2015). In this study, the invasion of pathogens was closely related to motility. The functional enrichment results of profile 43-PP showed that its genes were closely related to flagella (Figure 7). During infection, the genes in this module showed an upward trend until the fourth day, after which gene expression decreased slightly due to increased host death. Comprehensive GO enrichment and STEM results suggest that flagella are critical for pathogens in host infection. In the late stage of infection, pathogens are widely distributed in the host; therefore, the role of flagella may be slightly decreased, resulting in a decrease in the expression of related genes. Flagellar motility is an essential process in many phases of a pathogen's life cycle, and virulence and motility are often intimately linked by complex regulatory networks (Josenhans & Suerbaum, 2002). To date, flagella are known to be involved in the virulence of many aquatic pathogenic bacteria, such as *Yersinia ruckeri* (Jozwick et al., 2019), *Edwardsiella tarda* (Morimoto et al., 2019), *Aliivibrio salmonicida* (Nørstebø et al., 2017), and *Vibrio anguillarum* (Liu et al., 2014). In addition, the silencing of flagellum genes *fliA* and *figM* significantly reduces the pathogenicity of *P. plecoglossicida* (Sun et al., 2019a, 2019b).

Dual RNA-seq analysis evidenced the modulation of *P.*

plecoglossicida and *L. crocea* during infection. The WGCNA results showed that the relationship between host and pathogen was complex, and five pathogenic genes, i.e., *aldH*, *dapA*, *dadA*, *L321_RS03170*, and *L321_RS20070*, showed high correlation with the host immune response. These five genes are all related to the metabolic processes of bacteria (Figure 8C). The product dihydrodipicolinate synthase (DHDPS) encoded by the *dapA* gene is involved in the diaminopimelate (DAP) pathway, which yields essential metabolic building products, namely, meso-DAP and lysine (Dante et al., 1999; Motoyama et al., 2001). The essential amino acid L-lysine is an important precursor for the synthesis of the peptidoglycan cell wall, housekeeping proteins, and virulence factors of bacteria (Peverelli et al., 2016). DHDPS is the product of an essential bacterial gene and is a promising target for antibiotic development (Griffin et al., 2008). The *dapA* gene is critical in many bacterial species, including *Salmonella typhimurium* (Becker et al., 2006), *Bacillus subtilis* (Kobayashi et al., 2003), *Mycobacterium tuberculosis* (Shrivastava et al., 2016), and *Pseudomonas aeruginosa* (Impey et al., 2020). The *aldH* gene is associated with the aldehyde dehydrogenase (ALDH) superfamily, which is widely found in all kingdoms from archaea to mammals, including humans, and participates in a broad variety of metabolic pathways (Brocker et al., 2013; Jackson et al., 2015; Marchitti et al., 2008). The *Pseudomonas* genus contains many genes that encode ALDHs (Riveros-Rosas et al., 2019). Annotation of the *L321_RS20070* gene has shown that it is also closely related to aldehyde dehydrogenase. The enzyme encoded by *dadA* is also essential for many bacteria to decompose energy substances (Bardaweel et al., 2011; Li & Lu, 2016).

CONCLUSIONS

In this study, we successfully used tissue dual RNA-seq to simultaneously analyze the dynamics of gene expression changes of both host and pathogen in the context of eukaryotic and prokaryotic biological systems, yielding high-resolution transcriptome data. For *L. crocea*, both metabolic processes and the use of oxygen had strong impact during infection. WGCNA revealed the relationship between the metabolic processes and the entire immune process. For *P. plecoglossicida*, motility was the most important life activity during infection, and pathogen invasion exhibited strong dependence on flagella. This study represents the first use of a complex network inference model to infer molecular interspecies interactions between a bacterial pathogen and host (cells and tissues) and successfully predict key disease-causing genes. Application of the tools in more infection systems has dramatically expanded our potential ability to uncover complex pathogenic mechanisms at various periods of *in vivo* infection.

For future studies: (i) In all previous studies plus the present research, time-resolved dual RNA-seq of tissue studies have provided a first step for application of dual RNA-seq to *in vivo* models of infection. In the four cases, infected tissues were

homogenized prior to RNA extraction and sequencing. This finding means that the host fraction is composed of more than a single cell type. Thus, cell-type-specific tissue dual RNA-seq should be used in the future to increase the resolution of the experiment. (ii) The low bacterial burden in infected tissues and fluctuation of burden during different infectious periods is a limitation for time-resolved dual RNA-seq of tissue. Ongoing progress in sample processing and sequencing technologies provides a high-throughput time point (no limit of infection period) for dual RNA-seq of tissues and provides a more complete picture for understanding the mechanisms underlying bacterial *in vivo* infection. (iii) The feasibility of time-resolved dual RNA-seq of tissue will pose significant challenges for the bioinformatics analysis of resulting datasets, and future efforts will be needed to exploit their full potential.

Dual RNA-seq was used to identify simultaneous host and pathogen gene expression and their interactions associated with infection time in *L. crocea*. While gene expression is only one of the many biological processes involved, our findings add to a comprehensive understanding of bacterial diseases in fish and strongly suggest that neither host nor pathogen should be studied in isolation when possible. Many associations between gene expression and infection duration were identified, which should help to elucidate the pathogenesis of visceral white spot disease.

SUPPLEMENTARY DATA

Supplementary data to this article can be found online.

COMPETING INTERESTS

The authors declare that they have no competing interests.

AUTHORS' CONTRIBUTIONS

Q.P.Y., L.X.H. and Y.Q.S. designed the study. Q.P.Y. and L.X.H. supervised the analyses. G.X., L.M.Z. and W.Q.Z. performed fish experiment. G.X. cultivated the bacteria. Y.T. extracted DNA and RNA. Y.T., L.X.H., Y.X.Q., B.W. and N.L. performed bioinformatics analysis. Y.T. wrote the manuscript with the other authors' input. Q.P.Y., L.X.H. and Y.Q.S. revised the manuscript. All authors read and approved the final version of the manuscript.

REFERENCES

- Akdis M, Aab A, Altunbulakli C, Azkur K, Costa RA, Cramer R, Duan S, Eiwegger T, Eljaszewicz A, Ferstl R, Frei R, Garbani M, Globinska A, Hess L, Huitema C, Kubo T, Komlosi Z, Konieczna P, Kovacs N, Kucuksezzer UC, Meyer N, Morita H, Olzhausen J, O'Mahony L, Pezer M, Prati M, Rebane A, Rhyner C, Rinaldi A, Sokolowska M, Stanic B, Sugita K, Treis A, Van De Veen W, Wanke K, Wawrzyniak M, Wawrzyniak P, Wirz OF, Zakzuk JS, Akdis CA. 2016. Interleukins (from IL-1 to IL-38), interferons, transforming growth factor β , and TNF- α : receptors, functions, and roles in diseases. *Journal of Allergy and Clinical Immunology*, 138(4): 984–1010.

- Aprianto R, Slager J, Holsappel S, Veening JW. 2016. Time-resolved dual RNA-seq reveals extensive rewiring of lung epithelial and pneumococcal transcriptomes during early infection. *Genome Biology*, **17**: 198.
- Bardaweel S, Ghosh B, Chou TF, Sadowsky MJ, Wagner CR. 2011. *E. coli* histidine triad nucleotide binding protein 1 (echH1) is a catalytic regulator of D-alanine dehydrogenase (DadA) activity *in vivo*. *PLoS One*, **6**(7): e20897.
- Becker D, Selbach M, Rollenhagen C, Ballmaier M, Meyer TF, Mann M, Bumann D. 2006. Robust *Salmonella* metabolism limits possibilities for new antimicrobials. *Nature*, **440**(7082): 303–307.
- Billar JD, Takahashi LS. 2018. Oxidative stress and fish immune system: phagocytosis and leukocyte respiratory burst activity. *Anais da Academia Brasileira de Ciências*, **90**(4): 3403–3414.
- Brocker C, Vasiliou M, Carpenter S, Carpenter C, Zhang YC, Wang XP, Kotchoni SO, Wood AJ, Kirch HH, Kopečný D, Nebert DW, Vasiliou V. 2013. Aldehyde dehydrogenase (ALDH) superfamily in plants: gene nomenclature and comparative genomics. *Planta*, **237**(1): 189–210.
- Chaban B, Hughes HV, Beeby M. 2015. The flagellum in bacterial pathogens: for motility and a whole lot more. *Seminars in Cell & Developmental Biology*, **46**: 91–103.
- Chen JP, Pang W, Zhao ZW, Bi YH, Chen XW. 2019. Transcription profiles of skin and head kidney from goldfish suffering hemorrhagic septicemia with an emphasis on the TLR signaling pathway. *Zoological Research*, **40**(4): 337–342.
- Curti A, TrabANELLI S, Salvestrini V, Baccarani M, Lemoli RM. 2009. The role of indoleamine 2,3-dioxygenase in the induction of immune tolerance: focus on hematology. *Blood*, **113**(11): 2394–2401.
- Dante RA, Neto GC, Leite A, Yunes JA, Arruda P. 1999. The *DapA* gene encoding the lysine biosynthetic enzyme dihydrodipicolinate synthase from *Coix lacryma-jobi*: cloning, characterization, and expression analysis. *Plant Molecular Biology*, **41**(4): 551–561.
- Ernst J, Bar-Joseph Z. 2006. STEM: a tool for the analysis of short time series gene expression data. *BMC Bioinformatics*, **7**: 191.
- Ganeshan K, Chawla A. 2014. Metabolic regulation of immune responses. *Annual Review of Immunology*, **32**: 609–634.
- Griffin MDW, Dobson RCJ, Pearce FG, Antonio L, Whitten AE, Liew CK, Mackay JP, Trehwella J, Jameson GB, Perugini MA, Gerrard JA. 2008. Evolution of quaternary structure in a homotetrameric enzyme. *Journal of Molecular Biology*, **380**(4): 691–703.
- Grote A, Voronin D, Ding T, Twaddle A, Unnasch TR, Lustigman S, Ghedin E. 2017. Defining *Brugia malayi* and *Wolbachia* symbiosis by stage-specific dual RNA-seq. *PLoS Neglected Tropical Diseases*, **11**(3): e0005357.
- Gulati A, Kaur D, Krishna Prasad GVR, Mukhopadhyaya A. 2018. PRR function of innate immune receptors in recognition of bacteria or bacterial ligands. In: Chattopadhyay K, Basu SC. *Biochemical and Biophysical Roles of Cell Surface Molecules*. Singapore: Springer, 255–280.
- Huang LX, Wang L, Lin XZ, Su YQ, Qin YX, Kong WD, Zhao LM, Xu XJ, Yan QP. 2017. *mcp*, *aer*, *cheB*, and *cheV* contribute to the regulation of *Vibrio alginolyticus* (ND-01) adhesion under gradients of environmental factors. *MicrobiologyOpen*, **6**(6): e00517.
- Huang LX, Liu WJ, Jiang QL, Zuo YF, Su YQ, Zhao LM, Qin YX, Yan QP. 2018. Integration of transcriptomic and proteomic approaches reveals the temperature-dependent virulence of *Pseudomonas plecoglossicida*. *Frontiers in Cellular and Infection Microbiology*, **8**: 207.
- Huang LX, Zuo YF, Jiang QL, Su YQ, Qin YX, Xu XJ, Zhao LM, Yan QP. 2019. A metabolomic investigation into the temperature-dependent virulence of *Pseudomonas plecoglossicida* from large yellow croaker (*Pseudosciaena crocea*). *Journal of Fish Diseases*, **42**(3): 431–446.
- Impey RE, Panjikar S, Hall CJ, Bock LJ, Sutton JM, Perugini MA, Soares Da Costa TP. 2020. Identification of two dihydrodipicolinate synthase isoforms from *Pseudomonas aeruginosa* that differ in allosteric regulation. *The FEBS Journal*, **287**(2): 386–400.
- Jackson BC, Thompson DC, Charkoftaki G, Vasiliou V. 2015. Dead enzymes in the aldehyde dehydrogenase gene family: role in drug metabolism and toxicology. *Expert Opinion on Drug Metabolism & Toxicology*, **11**(12): 1839–1847.
- Jenner RG, Young RA. 2005. Insights into host responses against pathogens from transcriptional profiling. *Nature Reviews Microbiology*, **3**(4): 281–294.
- Ji C, Guo XY, Ren JF, Zu Y, Li WM, Zhang QH. 2019. Transcriptomic analysis of microRNAs-mRNAs regulating innate immune response of zebrafish larvae against *Vibrio parahaemolyticus* infection. *Fish & Shellfish Immunology*, **91**: 333–342.
- Josenshans C, Suerbaum S. 2002. The role of motility as a virulence factor in bacteria. *International Journal of Medical Microbiology*, **291**(8): 605–614.
- Jozwick AKS, LaPatra SE, Graf J, Welch TJ. 2019. Flagellar regulation mediated by the Rcs pathway is required for virulence in the fish pathogen *Yersinia ruckeri*. *Fish & Shellfish Immunology*, **91**: 306–314.
- Kanehisa M, Goto S. 2000. KEGG: Kyoto encyclopedia of genes and genomes. *Nucleic Acids Research*, **28**(1): 27–30.
- Ken CF, Chen CN, Ting CH, Pan CY, Chen JY. 2017. Transcriptome analysis of hybrid tilapia (*Oreochromis* spp.) with *Streptococcus agalactiae* infection identifies Toll-like receptor pathway-mediated induction of NADPH oxidase complex and piscidins as primary immune-related responses. *Fish & Shellfish Immunology*, **70**: 106–120.
- Kim D, Langmead B, Salzberg SL. 2015. HISAT: a fast spliced aligner with low memory requirements. *Nature Methods*, **12**(4): 357–360.
- Klopfenstein DV, Zhang L, Pedersen BS, Ramirez F, Warwick Vesztrocy A, Naldi A, Mungall CJ, Yunes JM, Botvinnik O, Weigel M, Dampier W, Dessimoz C, Flick P, Tang H. 2018. GOATOOLS: A Python library for Gene Ontology analyses. *Scientific Reports*, **8**(1): 10872.
- Kobayashi K, Ehrlich SD, Albertini A, Amati G, Andersen KK, Arnaud M, Asai K, Ashikaga S, Aymerich S, Bessieres P, Boland F, Brignell SC, Bron S, Bunai K, Chapuis J, Christiansen LC, Danchin A, Débarbouille M, Dervyn E, Deuerling E, Devine K, Devine SK, Dreesen O, Errington J, Fillinger S, Foster SJ, Fujita Y, Galizzi A, Gardan R, Eschevins C, Fukushima T, Haga K, Harwood CR, Hecker M, Hosoya D, Hullo MF, Kakeshita H, Karamata D, Kasahara Y, Kawamura F, Koga K, Koski P, Kuwana R, Imamura D, Ishimaru M, Ishikawa S, Ishio I, Le Coq D, Masson A, Mauël C, Meima R, Mellado RP, Moir A, Moriya S, Nagakawa E, Nanamiya H, Nakai S, Nygaard P, Ogura M, Ohanan T, O'Reilly M, O'Rourke M, Pragai Z, Pooley HM, Rapoport G, Rawlins JP, Rivas LA, Rivolta C, Sadaie A, Sadaie Y, Sarvas M, Sato T, Saxild HH, Scanlan E, Schumann W, Seegers JFML, Sekiguchi J, Sekowska A, Sérór SJ, Simon M, Stragier P, Studer R, Takamatsu H, Tanaka T, Takeuchi M, Thomaidis HB, Vagner V, Van Dijk JM, Watabe K, Wipat A, Yamamoto H, Yamamoto M, Yamamoto Y, Yamane K, Yata K, Yoshida K, Yoshikawa H, Zuber U, Ogasawara N. 2003. Essential *Bacillus subtilis* genes. *Proceedings of the National Academy of Sciences of the United States of America*, **100**(8): 4678–4683.

- Langfelder P, Horvath S. 2008. WGCNA: an R package for weighted correlation network analysis. *BMC Bioinformatics*, **9**: 559.
- Li B, Dewey CN. 2011. RSEM: accurate transcript quantification from RNA-Seq data with or without a reference genome. *BMC Bioinformatics*, **12**: 323.
- Li GQ, Lu CD. 2016. The cryptic *dsdA* gene encodes a functional D-serine dehydratase in *Pseudomonas aeruginosa* PAO1. *Current Microbiology*, **72**(6): 788–794.
- Liu PF, Du YS, Meng LJ, Li X, Liu Y. 2016. Metabolic profiling in kidneys of Atlantic salmon infected with *Aeromonas salmonicida* based on ¹H NMR. *Fish & Shellfish Immunology*, **58**: 292–301.
- Liu WJ, Huang LX, Su YQ, Qin YX, Zhao LM, Yan QP. 2017. Contributions of the oligopeptide permeases in multistep of *Vibrio alginolyticus* pathogenesis. *MicrobiologyOpen*, **6**(5): e00511.
- Liu XH, Wu HZ, Chang XY, Tang YF, Liu Q, Zhang YX. 2014. Notable mucosal immune responses induced in the intestine of zebrafish (*Danio rerio*) bath-vaccinated with a live attenuated *Vibrio anguillarum* vaccine. *Fish & Shellfish Immunology*, **40**(1): 99–108.
- Livak KJ, Schmittgen TD. 2001. Analysis of relative gene expression data using real-time quantitative PCR and the 2^{-ΔΔC_t} method. *Methods*, **25**(4): 402–408.
- Lu J, Shi YY, Cai SH, Feng JH. 2017. Metabolic responses of *Haliotis diversicolor* to *Vibrio parahaemolyticus* infection. *Fish & Shellfish Immunology*, **60**: 265–274.
- Lu XJ, Chen J. 2019. Specific function and modulation of teleost monocytes/macrophages: polarization and phagocytosis. *Zoological Research*, **40**(3): 146–150.
- Lulijwa R, Alfaro AC, Merien F, Meyer J, Young T. 2019. Advances in salmonid fish immunology: A review of methods and techniques for lymphoid tissue and peripheral blood leucocyte isolation and application. *Fish & Shellfish Immunology*, **95**: 44–80.
- Luo G, Xu XJ, Zhao LM, Qin YX, Huang LX, Su YQ, Yan QP. 2019a. *clpV* is a key virulence gene during in vivo *Pseudomonas plecoglossicida* infection. *Journal of Fish Diseases*, **42**(7): 991–1000.
- Luo G, Zhao LM, Xu XJ, Qin YX, Huang LX, Su YQ, Zheng WQ, Yan QP. 2019b. Integrated dual RNA-seq and dual iTRAQ of infected tissue reveals the functions of a diguanylate cyclase gene of *Pseudomonas plecoglossicida* in host-pathogen interactions with *Epinephelus coioides*. *Fish & Shellfish Immunology*, **95**: 481–490.
- Luo G, Sun YJ, Huang LX, Su YQ, Zhao LM, Qin YX, Xu XJ, Yan QP. 2020. Time-resolved dual RNA-seq of tissue uncovers *Pseudomonas plecoglossicida* key virulence genes in host-pathogen interaction with *Epinephelus coioides*. *Environmental Microbiology*, **22**(2): 677–693.
- Marchitti SA, Brocker C, Stagos D, Vasiliou V. 2008. Non-P450 aldehyde oxidizing enzymes: the aldehyde dehydrogenase superfamily. *Expert Opinion on Drug Metabolism & Toxicology*, **4**(6): 697–720.
- Minhas V, Aprianto R, McAllister LJ, Wang H, David SC, McLean KT, Comerford I, McColl SR, Paton JC, Veening JW, Trappetti C. 2019. In vivo dual RNA-Seq analysis reveals the basis for differential tissue tropism of clinical isolates of *Streptococcus pneumoniae*. *bioRxiv*, doi: 10.1101/862755.
- Mondanelli G, Iacono A, Allegrucci M, Puccetti P, Grohmann U. 2019. Immunoregulatory interplay between arginine and tryptophan metabolism in health and disease. *Frontiers in Immunology*, **10**: 1565.
- Morimoto N, Kondo M, Kono T, Sakai M, Hikima JI. 2019. Nonconservation of TLR5 activation site in *Edwardsiella tarda* flagellin decreases expression of interleukin-1β and NF-κB genes in Japanese flounder, *Paralichthys olivaceus*. *Fish & Shellfish Immunology*, **87**: 765–771.
- Motoyama H, Yano H, Terasaki Y, Anazawa H. 2001. Overproduction of L-Lysine from methanol by *Methylobacillus glycogenes* derivatives carrying a plasmid with a mutated *dapA* gene. *Applied and Environmental Microbiology*, **67**(7): 3064–3070.
- Nhan JD, Turner CD, Anderson SM, Yen CA, Dalton HM, Cheesman HK, Ruter DL, Uma Naresh N, Haynes CM, Soukas AA, Pukkila-Worley R, Curran SP. 2019. Redirection of SKN-1 abates the negative metabolic outcomes of a perceived pathogen infection. *Proceedings of the National Academy of Sciences of the United States of America*, **116**(44): 22322–22330.
- Nishimori E, Kita-Tsukamoto K, Wakabayashi H. 2000. *Pseudomonas plecoglossicida* sp. nov., the causative agent of bacterial haemorrhagic ascites of ayu, *Plecoglossus altivelis*. *International Journal of Systematic and Evolutionary Microbiology*, **50**(1): 83–89.
- Nørstebø SF, Paulshus E, Bjelland AM, Sørum H. 2017. A unique role of flagellar function in *Aliivibrio salmonicida* pathogenicity not related to bacterial motility in aquatic environments. *Microbial Pathogenesis*, **109**: 263–273.
- Peverelli MG, Soares da Costa TP, Kirby N, Perugini MA. 2016. Dimerization of bacterial diaminopimelate decarboxylase is essential for catalysis. *Journal of Biological Chemistry*, **291**(18): 9785–9795.
- Ritchie ND, Evans TJ. 2019. Dual RNA-seq in *Streptococcus pneumoniae* infection reveals compartmentalized neutrophil responses in lung and pleural space. *mSystems*, **4**(4): e00216–19.
- Riveros-Rosas H, Julián-Sánchez A, Moreno-Hagelsieb G, Muñoz-Clares RA. 2019. Aldehyde dehydrogenase diversity in bacteria of the *Pseudomonas* genus. *Chemico-Biological Interactions*, **304**: 83–87.
- Shrivastava P, Navratna V, Silla Y, Dewangan RP, Pramanik A, Chaudhary S, Rayasam G, Kumar A, Gopal B, Ramachandran S. 2016. Inhibition of *Mycobacterium tuberculosis* dihydrodipicolinate synthase by alpha-ketopimelic acid and its other structural analogues. *Scientific Reports*, **6**: 30827.
- Sorek R, Cossart P. 2010. Prokaryotic transcriptomics: a new view on regulation, physiology and pathogenicity. *Nature Reviews Genetics*, **11**(1): 9–16.
- Sun YJ, Luo G, Zhao LM, Huang LX, Qin YX, Su YQ, Yan QP. 2018. Integration of RNAi and RNA-seq reveals the immune responses of *Epinephelus coioides* to *sigX* gene of *Pseudomonas plecoglossicida*. *Frontiers in Immunology*, **9**: 1624.
- Sun YJ, Nie P, Zhao LM, Huang LX, Qin YX, Xu XJ, Zhang JN, Yan QP. 2019a. Dual RNA-Seq unveils the role of the *Pseudomonas plecoglossicida* *fliA* gene in pathogen-host interaction with *Larimichthys crocea*. *Microorganisms*, **7**(10): 443.
- Sun YJ, Zhuang ZX, Wang XR, Huang HB, Fu Q, Yan QP. 2019b. Dual RNA-seq reveals the effect of the *flgM* gene of *Pseudomonas plecoglossicida* on the immune response of *Epinephelus coioides*. *Fish & Shellfish Immunology*, **87**: 515–523.
- Tang RQ, Luo G, Zhao LM, Huang LX, Qin YX, Xu XJ, Su YQ, Yan QP. 2019a. The effect of a LysR-type transcriptional regulator gene of *Pseudomonas plecoglossicida* on the immune responses of *Epinephelus coioides*. *Fish & Shellfish Immunology*, **89**: 420–427.

- Tang RQ, Zhao LM, Xu XJ, Huang LX, Qin YX, Su YQ, Yan QP. 2019b. Dual RNA-Seq uncovers the function of an ABC transporter gene in the host-pathogen interaction between *Epinephelus coioides* and *Pseudomonas plecoglossicida*. *Fish & Shellfish Immunology*, **92**: 45–53.
- Tang Y, Sun YJ, Zhao LM, Xu XJ, Huang LX, Qin YX, Su YQ, Yi GF, Yan QP. 2019c. Mechanistic insight into the roles of *Pseudomonas plecoglossicida* *clpV* gene in host-pathogen interactions with *Larimichthys crocea* by dual RNA-seq. *Fish & Shellfish Immunology*, **93**: 344–353.
- Tao Z, Zhou T, Zhou SM, Wang GL. 2016. Temperature-regulated expression of type VI secretion systems in fish pathogen *Pseudomonas plecoglossicida* revealed by comparative secretome analysis. *FEMS Microbiology Letters*, **363**(22): fnw261.
- Thänert R, Goldmann O, Beineke A, Medina E. 2017. Host-inherent variability influences the transcriptional response of *Staphylococcus aureus* during *in vivo* infection. *Nature Communications*, **8**: 14268.
- Wang LY, Sun YJ, Zhao LM, Xu XJ, Huang LX, Qin YX, Su YQ, Zhang JN, Yan QP. 2019. Dual RNA-seq uncovers the immune response of *Larimichthys crocea* to the *secY* gene of *Pseudomonas plecoglossicida* from the perspective of host-pathogen interactions. *Fish & Shellfish Immunology*, **93**: 949–957.
- Westermann AJ, Gorski SA, Vogel J. 2012. Dual RNA-seq of pathogen and host. *Nature Reviews Microbiology*, **10**(9): 618–630.
- Westermann AJ, Förstner KU, Amman F, Barquist L, Chao YJ, Schulte LN, Müller L, Reinhardt R, Stadler PF, Vogel J. 2016. Dual RNA-seq unveils noncoding RNA functions in host–pathogen interactions. *Nature*, **529**(7587): 496–501.
- Westermann AJ, Barquist L, Vogel J. 2017. Resolving host-pathogen interactions by dual RNA-seq. *PLoS Pathogens*, **13**(2): e1006033.
- Yang J, Lu XJ, Chai FC, Chen J. 2016. Molecular characterization and functional analysis of a piscidin gene in large yellow croaker (*Larimichthys crocea*). *Zoological Research*, **37**(6): 347–355.
- Yang Y, Adeola AC, Xie HB, Zhang YP. 2018. Genomic and transcriptomic analyses reveal selection of genes for puberty in Bama Xiang pigs. *Zoological Research*, **39**(6): 424–430.
- Yilmaz E. 2019. Effects of dietary anthocyanin on innate immune parameters, gene expression responses, and ammonia resistance of Nile tilapia (*Oreochromis niloticus*). *Fish & Shellfish Immunology*, **93**: 694–701.
- Yin F, Dan XM, Sun P, Shi ZH, Gao QX, Peng SM, Li AX. 2014. Growth, feed intake and immune responses of orange-spotted grouper (*Epinephelus coioides*) exposed to low infectious doses of ectoparasite (*Cryptocaryon irritans*). *Fish & Shellfish Immunology*, **36**(1): 291–298.
- Yin F, Gong H, Ke QZ, Li AX. 2015. Stress, antioxidant defence and mucosal immune responses of the large yellow croaker *Pseudosciaena crocea* challenged with *Cryptocaryon irritans*. *Fish & Shellfish Immunology*, **47**(1): 344–351.
- Yu GC, Wang LG, Han Y, He QY. 2012. clusterProfiler: an R package for comparing biological themes among gene clusters. *OMICS*, **16**(5): 284–287.
- Zhang BB, Luo G, Zhao LM, Huang LX, Qin YX, Su YQ, Yan QP. 2018a. Integration of RNAi and RNA-seq uncovers the immune responses of *Epinephelus coioides* to *L321_RS19110* gene of *Pseudomonas plecoglossicida*. *Fish & Shellfish Immunology*, **81**: 121–129.
- Zhang BB, Zhuang ZX, Wang XR, Huang HB, Fu Q, Yan QP. 2019a. Dual RNA-Seq reveals the role of a transcriptional regulator gene in pathogen-host interactions between *Pseudomonas plecoglossicida* and *Epinephelus coioides*. *Fish & Shellfish Immunology*, **87**: 778–787.
- Zhang JT, Zhou SM, An SW, Chen L, Wang GL. 2014. Visceral granulomas in farmed large yellow croaker, *Larimichthys crocea* (Richardson), caused by a bacterial pathogen, *Pseudomonas plecoglossicida*. *Journal of Fish Diseases*, **37**(2): 113–121.
- Zhang M, Li L, Liu Y, Gao XL. 2019b. Effects of a sudden drop in salinity on immune response mechanisms of *Anadara kagoshimensis*. *International Journal of Molecular Sciences*, **20**(18): 4365.
- Zhang MM, Yan QP, Mao LL, Wang SY, Huang LX, Xu XJ, Qin YX. 2018b. *KatG* plays an important role in *Aeromonas hydrophila* survival in fish macrophages and escape for further infection. *Gene*, **672**: 156–164.
- Zhang MM, Qin YX, Huang LX, Yan QP, Mao LL, Xu XJ, Wang SY, Zhang MM, Chen LW. 2019c. The role of *sodA* and *sodB* in *Aeromonas hydrophila* resisting oxidative damage to survive in fish macrophages and escape for further infection. *Fish & Shellfish Immunology*, **88**: 489–495.